PRELIMINARY DISCRETE MODELLING OF LANDFILLS CLAY BARRIER

Jean-Pierre Gourc, Olivier Ple, Pascal Villard

PRELIMINARY DISCRETE MODELLING OF LANDFILLS CLAY BARRIER

JEAN-PIERRE GOURC*, OLIVIER PLE**, PASCAL VILLARD**

**Laboratoire THE, Université Joseph Fourier de Grenoble, Domaine Universitaire, B.P. 53, F-38041 Grenoble cedex 9, France*
***Laboratoire 3S-R, Université Joseph Fourier de Grenoble, Domaine Universitaire, B.P. 53, F-38041 Grenoble cedex 9, France*

SUMMARY: The Discrete Element Method is used to investigate the tensile behaviour and cracks mechanisms of a clay material submitted to bending loading. It is the case of compacted clay liners in landfill cap cover application. Such as the soil tested in this study is plastic clay, the distinct elements model was calibrated with previous data results by taking into account cohesive properties. Various contact and cohesion laws are tested to show that the numerical model is able to reproduce the failure mechanism. Numerical results are extending to simulate a landfill cap cover.

1. INTRODUCTION

Landfills have a top barrier including, in particular, a cap cover of compacted clay layer. However, this barrier poses many problems, in particular related to its in situ implementation and during exploitation as mechanical loading which can induce cracks into the clay layer.

Then, it is necessary to keep at required level physical and mechanical characteristics of the cover barrier to guarantee waterproofing properties and the safety of the site. Constitutive laws for compressive or shearing strength are proposed in the literature but tensile strength of the clay material is poorly investigated. As experiments are difficult to conduct a solution with discrete element modelling can be proposed as new alternative.

Already developed to model the total behaviour of grains (Cundall and Strack, 1979), this method is classically not used to take into account the tensile behaviour of cohesive material. Such as the soil tested in the study is plastic clay, the distinct elements method is first calibrated with the reference law of PFC²D code and applied to simulate a biaxial experiment.

Various contact, friction and cohesion laws are tested to understand how interactions between particles are related to the macroscopic parameters of the clay material tested.

Extensions to the tensile strength are done and show that the numerical simulation is able to reproduce the failure mechanism observed in laboratory.

An application of this approach regarding a cap cover of a landfill barrier is done.

2. EXPERIMENTAL PROCEDURE

The influence of differential settlements within the waste mass on the capping cover is experimentally modeled by submitting a clay layer to bending stresses. Bursting tests (Figure 1) have been selected in order to be in position to observe the initialization of cracks.

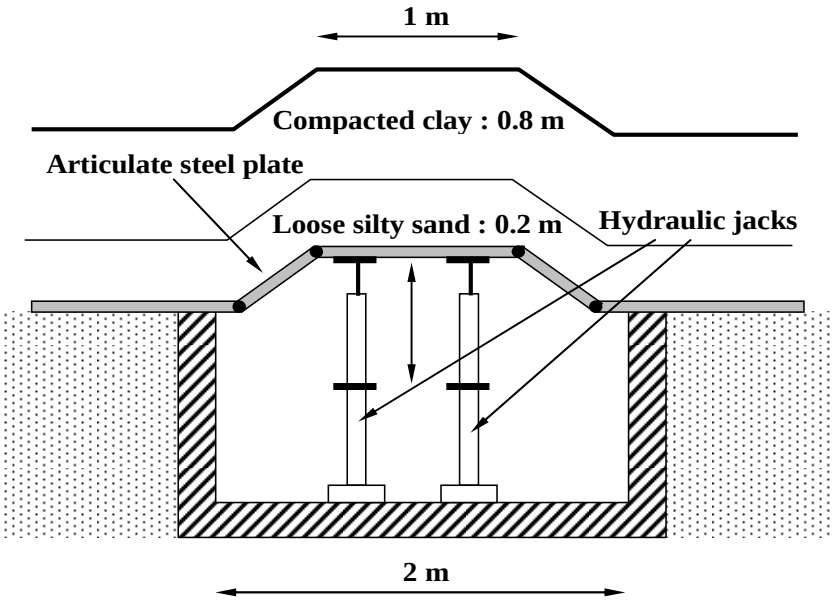

Figure 1. Bursting test on a capping cover.

For the implementation of this test, a rigid pit in reinforced concrete (width of 2m) is built, and an articulated steel plate (2m × 2m) placed over the pit (Figure 1).

Plane strain state is considered as existing for a central profile. A system of four hydraulic jacks in the pit allows the plate to reproduce local upthrust (Figure 1). The jacks are synchronized to ensure the same displacement of the four corners of the plate and an equal load on each jack. A series of displacement transducers and load cells monitor the jacks. The maximal vertical displacement of the plate is 0.25 m. At first non compacted silty sand is implemented under a compacted clay layer (Figure 1). Experimental results coming from a field bending test (Camp, 2008) show, for a real case of plastic clay, that the tensile strength is very sensitive to deflection.

The first crack appears in the axial part for a displacement of the plate equal to 2 cm. At the end of the test (displacement of 25 cm, loading 42 kN/m²) a cut is realized (Figure 2).

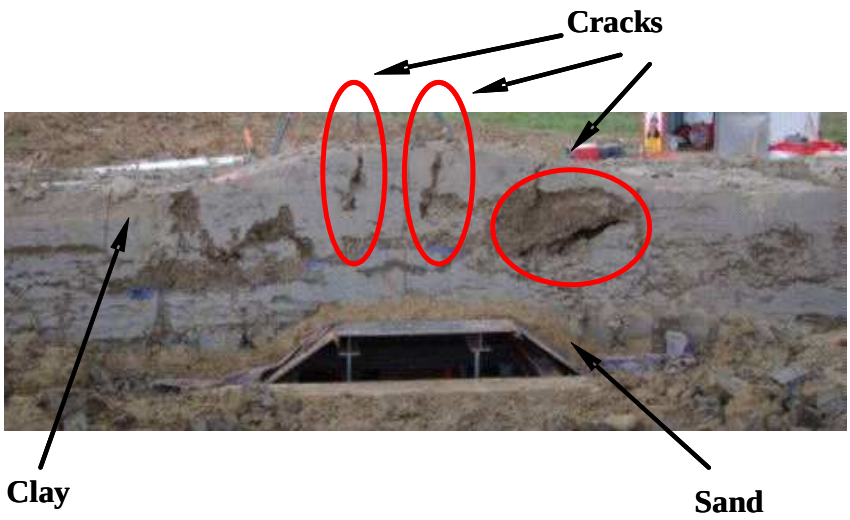

Figure 2. Field test on the cap cover (displacement of the plate of 25 cm).

Laboratory triaxial tests of characterisation are performed on both materials (clay and sand) to reproduce the conditions of in situ implementation (>w_{opn}) and exploitation on site. Interpretation is carried out in terms of total stresses. The results enable Mohr-Coulomb circles to be determined and cohesion parameter (C) and friction angle (ϕ) to be deducted (Table 1).

For the clay and for high water content values, ranging between the Proctor optimum (w_{opn}) and w_{opn} + 4%, the experimental tests are considered intermediate tests between undrained and unconsolidated tests (U.U. tests) and undrained and consolidated tests (C.U. tests).

The sand can be considered as a purly friction material without cohesion. Previous experimental results on it enable the rigidity to be estimated.

Unconfined compression tests are performed on clay material. Under these conditions the clay can be characterized by a rigidity (the Young modulus, under uniaxial compression tests: E_{app}) and by a maximum stress. As the stress-strain curves are non-linear from the onset of loading, the rigidity is calculated with regard to the initial tangent modulus (Table 1). The peak of the stress-strain curves under uniaxial compression loading is retained for the compression strength (R_c).

Within the framework of this project, particular attention will be paid to experimental results by focussing our analysis on the failure process. To do this, the limit value of the extension strain of the material without crack development should be considered. In the in situ implementation conditions of a cap cover materials can be subjected to deformations. So, experimental results, on tensile strength are necessary for a continuum modelling of a cap cover and especially for the clay layer. These results could be obtained under direct tensile tests or splitting tests on clay. In all cases, the value of the stress at the initiation of crack is called the tensile strength (R_t). For reasons of simplicity splitting tests on clay are conducted in laboratory. Curves obtained present a preliminary relatively linear part which is characterized by a stiffness. Cracks appear generally at the end of the linear part of the behaviour. Taking into account the preceding remarks and from interpretation based on linear elasticity, R_t can be estimated under the form:

$$R_t = 2F/(D \times H \times \pi) \quad (1)$$

where F is the load at the crack initiation.

The parameters resulting from tests of characterization on clay and silty sand are collected in Table 1.

Table 1. Macroscopique parameters of the cap cover.

	Clay	Sand
R_c (kPa)	170	/
R_t (kPa)	10	0
E_{app} (MPa)	3	13
ϕ (°)	3	31
C (kPa)	80	0

With R_c the compression strength, R_t the tensile strength, E_{app} the Young modulus, ϕ the undrained apparent friction angle and C the undrained apparent cohesion.

3. NUMERICAL PROCEDURE

The numerical sample is built by the ERDF (Expansion de Rayon de Diminution de Frottement) method developed by Chareyre and Villard (2003). Samples are limited by a given volume. Particles are generated randomly inside the volume with a size reduced. No friction is taken into account between discs and boundaries. The size of particles is growing up until the sample reaches required porosity noted n. Micromechanical parameters of the model are selected to test samples under different loading. We use six micromechanical parameters:

- k_n and k_s (normal and tangential stiffness),
- a_n and a_s (normal and tangential adherence),
- n (porosity of samples),
- μ (the coefficient of friction between two discs).

The interaction between two particles (Figure 3) is made by resulting loading coming from a normal force F_n and a tangential force F_s at each step of time i under the form:

$$F_i = F_i^n + F_i^s \tag{2}$$

$$F_i^n = k_n U_n \tag{3}$$

$$\Delta F_i^s = k_s \Delta U_s \tag{4}$$

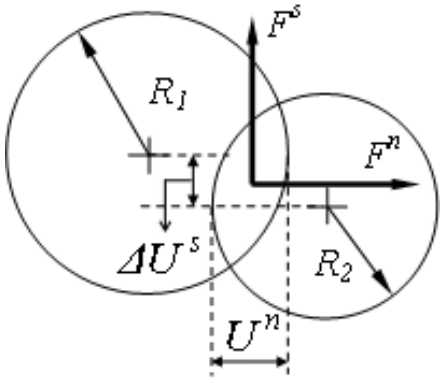

Figure 3. Interaction between particles.

U_n and ΔU_s are respectively relative displacements in the normal and shear directions. R_1 and R_2 represent the radius of discs.

3.1 Silty sand modelling

In order to reproduce the macroscopic behaviour of the loose sand, the granular assembly is made of clusters setting up at a low density. Each cluster is an assembly of two inseparable jointed discs with diameters D and $0.9 \times D$. The sample is built with two sizes of clusters. The ratio between the big one and the little one is equal to 2 and proportion between them is equal to 50%. The macroscopic parameters of the sand are obtained using samples of 5000 clusters submitted to various biaxial loading. Values of the microscopic parameters needed to reproduce the behaviour of the silty sand are presented in Table 2.

Table 2. Microscopic parameters of the silty sand.

k_n (kN/m)	$52.8.10^3$
k_s (kN/m)	$26.4.10^3$
a_n (kN/m)	0
a_s (kN/m)	0
n (%)	20.15
μ	0.455

The resulting macroscopic behaviour characteristic of the loose sand (no pick value) is represented on the Figure 4 where σ is the normal stress and P is the confining pressure. The results enable Mohr-Coulomb circles to be determined and cohesion parameter (C) and friction angle (ϕ) to be deducted (Figure 5).

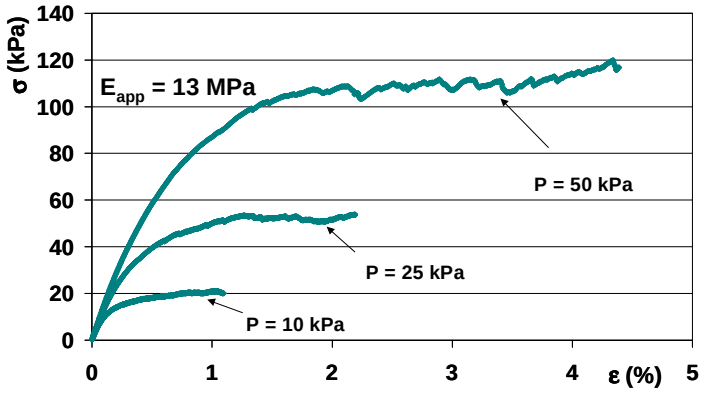

Figure 4. Simulation of biaxial tests on sand.

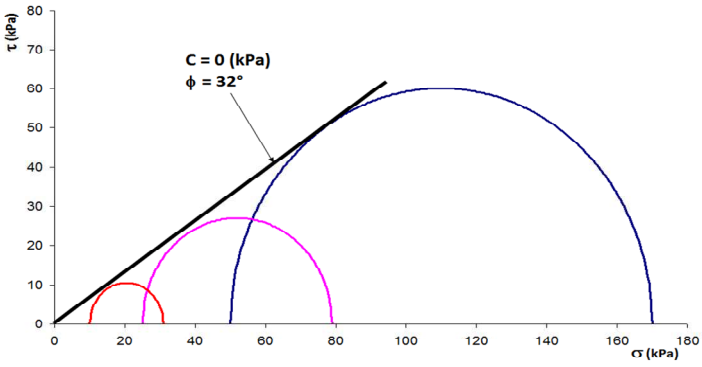

Figure 5. Mohr-Coulomb circles and intrinseque curve.

3.2 Contact laws and rupture criterion of the clay

The main macroscopic parameters which have an influence on cracks mechanism are the tensile strength and the Young modulus. The main numerical difficulties are link to the determination of the microscopic parameters which must simulate simultaneously direct tensile test and compression test into the clay layer. That's why the reference contact law proposed by PFC²D has been improved. In the initial configuration of PFC²D, the failure criterion, written as a function of failure by tension and failure by shearing, can be expressed under the form:

$$F_n > C_n \tag{5}$$

for the tensile failure.

In this expression $C_n = a_n \times D_{min}/2$ represents the ultimate normal cohesion. For the shearing failure the criterion can be written under the form:

$$F_s < Max\{C_s; F_n.\mu\} \tag{6}$$

where $C_s = a_s \times D_{min}/2$ is the ultimate tangential cohesion.

When contacts are failed, cohesions are lost. This simple contact behaviour is generally used for granular matter. To take into account the nature of the material tested (cohesive clay), we proposed an improvement of the shearing failure criterion under three ways. The first one can be expressed under the form:

$$F_s < C_s + F_n.\mu \tag{7}$$

Like in the reference law, the cohesion is lost when the contact is failed. The friction between two particles is always kept. This law will be noted law number 1. The second one can be expressed under the form:

$$F_s < Max(C_s; F_n.\mu) \tag{8}$$

When the failure criterion is reached, the cohesion is kept. We are dealing with a friction and a cohesive material. This law will be noted law number 2. Finally the third one where an addition between the cohesion and the friction is done under the form:

$$F_s < C_s + F_n.\mu \quad (9)$$

When the failure criterion is reached, the cohesion is kept. We are dealing with a friction and a cohesive material. The law will be note law number 3. In the following, the same sample of 5000 discs will be tested under different loading (uniaxial compression tests, axi-symmetric triaxial tests and direct tensile tests). Each granular assembly is made of discs with various diameters ranging between D_{min} and D_{max} (D_{max} / D_{min} = 3) setting up at porosity n.

In order to compare the different laws of contact, new numerical simulations are carried out, with the microscopic parameters given in Table 3. The Figure 6 shows the evolution of stresses and strains of a sample for different contact laws. It should be noted that the tensile strength is not influenced by the different contact laws. The maximum compression stress is in the range of 195 kPa to 368 kPa, i.e. in a ratio equal to 1.88. The corresponding strain is in the range of 2.48 % to 4.72 % showing a relative influence of the contact laws.

Table 3. Microscopic parameters of the clay.

k_n (kN/m)	20.10^3
k_s (kN/m)	20.10^3
a_n (kN/m)	400
a_s (kN/m)	400
n (%)	15.9
μ	0.2

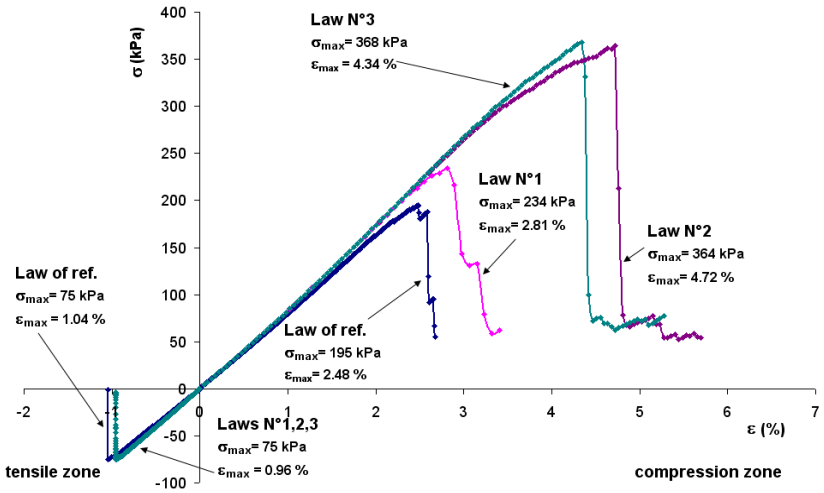

Figure 6. Tensile and compressive tests.

A numerical study was performed in order to obtain the microscopic parameters needed to reproduce the clay behaviour. A particular attention was paid to fit the Young modulus, the tensile strength and the ratio R_c/R_t. It should be noted that the rigidity of the sample (E_{app}) is directly link to the stiffness parameters. Relation between both is linear. A weak rigidity returns a more soft material. For a_n and a_s values, it should be noted that the direct tensile strength is not influenced by the microscopic tangential adherence. On the other hand, the direct tensile strength decreases when the local microscopic normal adherence decreases. The micromechanical parameters retained for the clay layer are those given in Table 4. The contact law used it law number 2.

Table 4. Micromechanical parameters of the cap cover.

k_n (kN/m)	10.10^3
k_s (kN/m)	10.10^3
a_n (kN/m)	100
a_s (kN/m)	400
n (%)	15.93
μ	0.2

3. APPLICATION TO A REAL CASE

For the silty sand, the numerical granular assembly is made of 2000 clusters. For the clay, the granular assembly is made of 8000 discs. The numerical geometry is similar to the real case. Particles are set up at a given porosity by using the ERDF method. The particles are subjected to gravity and then stabilized just before the simulation. The boundaries conditions of the numerical modelling are obtained by walls. Bursting test is obtained by the displacement of the horizontal wall at a constant speed rate. The resulting loading is measured continuously. Images of the simulation are used to analyze the damage process (Figure 8 and Figure 9).

The curve of the loading of the plate versus the vertical displacement is presented in Figure 7. The vertical ascending branch of the curve corresponds to the weight of the materials. The linear part of the curve corresponds to the elastic behaviour of the model. At the end of the linear part of the curve the first crack appears (Figure 8). The final part of the curve corresponds to the propagation of the crack into the clay layer. The maximum load (Figure 7) is obtained when cracks form distinct blocks. The propagation of cracks is represented on Figures 8 and 9. Numerical results are in good accordance with experimental observations. The initialisation of the first crack (Figure 8) corresponds to a displacement of the plate equal to 1.7 cm again 2 cm in the field test. At the end of the tests, resulting loading are in the same order (40 kN/m² again 42 kN/m² in the field test). Moreover, damage mechanisms are very similar (Figure 9) with a tensile crack in the middle part of the clay layer and shearing damage around. No crack is observed in the silty sand layer (Figure 2 and Figure 9).

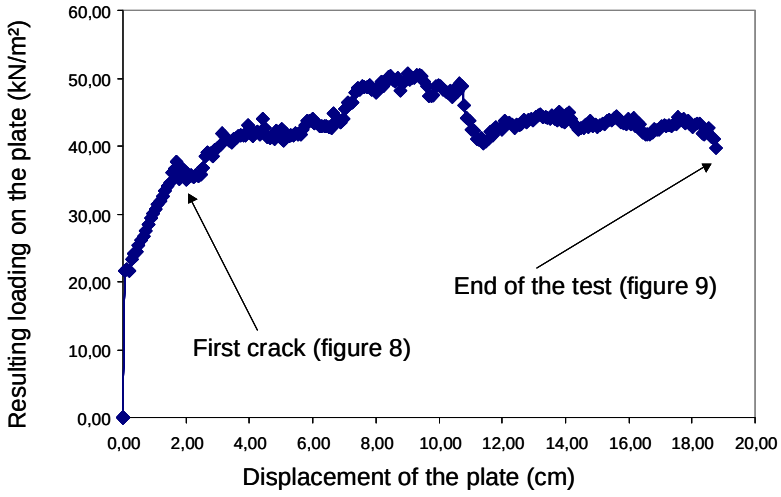

Figure 7. Numerical simulation of the burst field test.

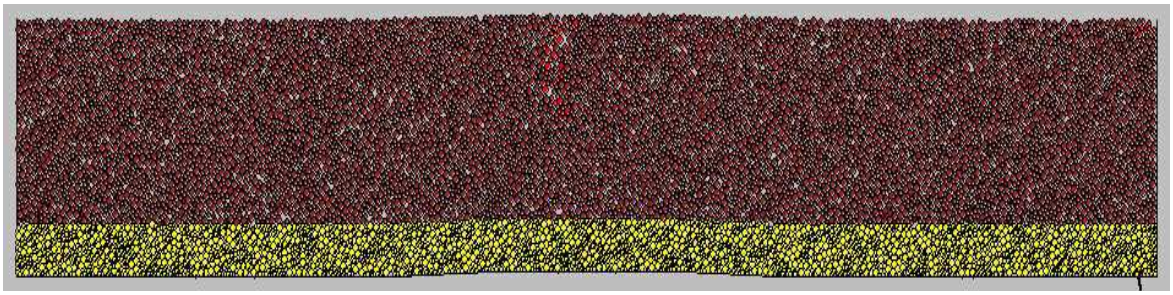

Figure 8. Initialization of the first crack (red particles).

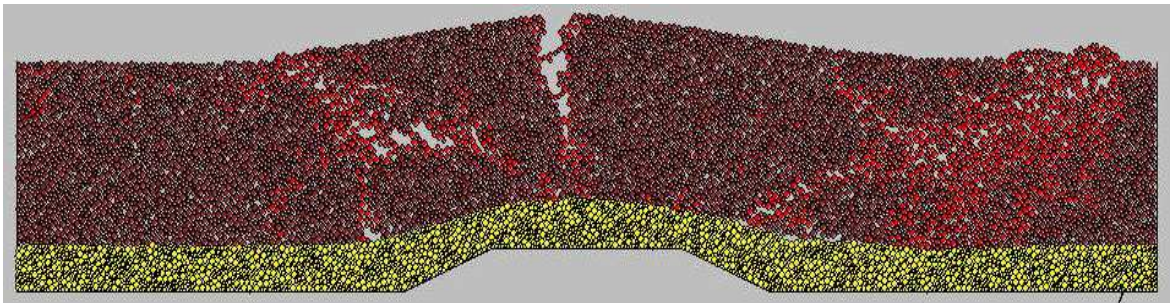

Figure 9. End of the simulation (displacement = 19 cm).

3. CONCLUDING REMARKS

Experimental studies on unsaturated clay are difficult to lead. A numerical approach using a discrete method is proposed. Different contact laws are used to describe the behaviour of a cohesive material. This first approach allows the simulation of a plastic clay under tensile tests. The numerical results are in good accordance with experimental data and make it possible to consider the simulation of a cap cover of composite materials under deflection.

REFERENCES

P.A. Cundall, O.D.L. Strack, 1979, A discrete numerical modelling method for granular assemblies, Geotechnique, 1979, 29, 1, p. 47-65.

B. Chareyre, P. Villard, 2003, Discret element modeling of curved geosynthetic anchorages with known macro-properties, 1er Inter. PFC Symp. (Gelsenkitchen, Germany, 6/7-11-2002), Konietzky (ed), p. 197-203.

S. Camp-Devernay 2008, Comportement sous flexion d'une argile: application à la couverture d'une ISD TFA, Ph-D thesis, Université Joseph Fourier, 350 p.